

Relation between total degradation of steel concrete bond and degree of corrosion of RC beams experimental and computational studies

Olivier Maurel[†]

Université de Reims, Champagne - Ardenne, France

Mickael Dekoster[‡] and François Buyle-Bodin^{‡‡}

*Université des Sciences et Technologies de Lille, USTL-LML, Cité Scientifique, 59655 Villeneuve d'Ascq, France
(Received March 16, 2004, Accepted January 30, 2005)*

Abstract. This paper presents a study on the effects of localized steel-concrete bond degradation on the flexural behaviour of RC beams. A finite element analysis is undertaken to complete the experimental analysis. The first part deals with an experimental study on beams where bond was removed by using plastic tube at different locations and for various lengths. The flexural behaviour was studied at global scale (load-deflection) and local scale (moment-curvature). The second part, a numerical study using a simplified special finite element (rust element) modelling the rust layer occurring between reinforcement and concrete with corrosion was conducted in order to find the relation between the degree of corrosion and the degradation of the steel-concrete bond. The computed value of the corrosion degree corresponding to the total degradation of bond has been used in a second time to model the tests, in order to evaluate the influence of the loss of bond, the steel cross section reduction, and the combination of both. The results enable to evaluate the influence of the different corrosion effects on the flexural behaviour, according to the length and the location of the corroded zone.

Keywords: reinforced concrete; reinforcement corrosion; steel-concrete bond; rust element.

1. Introduction

The corrosion of reinforcement is one of the main processes of degradation of reinforced concrete structures. The propagation of the corrosion starts when the steel is depassivated. Two situations mainly cause depassivation: the carbonation of the concrete cover followed by a uniformly distributed corrosion along the reinforcement, and a high concentration of chloride generating corrosion pitting. When the corrosion is propagating, the mechanical performances of RC structures begin to decrease. The sound steel cross section is reduced with the increase of corrosion degree. The production of rust on the bar surface causes an increase of the global volume (steel and rust) and induces supplementary stress on the cover concrete. The resulting degradation of the steel-

[†] Assistant Professor, E-mail: olivier.maurel@univ-reims.fr

[‡] Ph. D., E-mail: mickael.dekoster@segime.com

^{‡‡} Professor, Corresponding Author, E-mail: francois.buyle-bodin@univ-lille1.fr

concrete interface leads to the decrease of the steel-concrete bond.

The loss of steel cross section can be related with the decrease of the ultimate load, but leads to an underestimation of the flexural stiffness of the corroded beam. To correctly evaluate the influence of the corrosion on the mechanical behaviour, the loss of the steel cross section must be taken into account along with the degradation of the steel-concrete bond. The use of a special element equivalent to the rust layer seems to be an efficient solution (Dekoster, *et al.* 2003). But uniform corrosion has been more experimentally studied than localised corrosion. Few experimental studies are available concerning the behaviour of bending beams under localised corrosion. Almussalam, *et al.* (1996) has worked on concrete slabs, Lee, *et al.* (1998) on beams under flexure, Amleh and Mirza (1999) on tension test and Al-Sulaimani, *et al.* (1990) and Cabrera (1996) on pullout test and beam test. One study deals with heterogeneously localized corrosion on beams under flexure (Castel, *et al.* 2000). From all these studies, it is difficult to assess the effects of corrosion on a limited length of the longitudinal reinforcement. Moreover, the effects of corrosion variation along the longitudinal reinforced bar has never been taken into account. So, in this study, it has been chosen to experimentally analyse the effect of a total loss of bond on localized parts of longitudinal reinforcement of beams. The bond has been removed by encasing the bars in a plastic tube. The tests are made without reduction of the steel cross section. Then, using a Finite Element calculation, the relation between the total loss of bond and the corresponding degree of corrosion is established. Finally, simulations are conducted with the same FE method for a degree of corrosion equivalent to the total loss of bond considering the combination with the steel cross section reduction. The influence of both factors can thus be approached.

2. Experimental study

2.1. Materials and specimens description

The experiments were conducted on three beams where the steel-concrete bond was removed at various locations and for various lengths by surrounding the reinforcing longitudinal bars with a

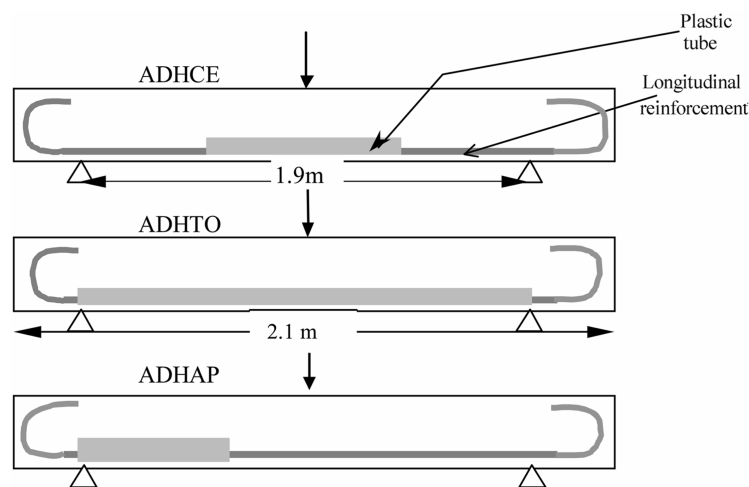


Fig. 1 Removed bond at different zones of the RC beams

plastic tube (Fig. 1). The bond of the stirrups and of the bars located at the compressed part of the beam was not modified. For the first beam, (called ADHCE) the bond was removed at mid-span, between the coordinates -40 cm and +40 cm compared to the mid-span of the beam. For the second beam, (called ADHTO) the bond was removed all along the longitudinal bars except along hooked ends and bearings. For the third beam, (called ADHAP) the bond was removed near one of the bearings between the coordinates -35 cm and -95 cm. A fourth beam (called TEMOIN) was tested as a control beam. The length of the beams was 2.1 m with a cross section of $150 \times 280 \text{ mm}^2$. Geometrical characteristics of the cross section are presented in Fig. 2. The average value of the tensile strength of the concrete at 28 days was 4.1 MPa. The average value of the compressive strength at 28 days was 32.7 MPa. The yield strength of the 12 mm diameter longitudinal steel bars was 550 MPa. Shear reinforcement consisted of 6 mm stirrups with 100 mm spacing throughout two-thirds of the beam.

For the three point flexural tests, the way of loading is presented in Fig. 3, with a first loading at 20 kN, followed by an unloading, then a second loading at 30 kN and a new unloading, then an increasing loading until failure. This load pattern was used to register residual deflections after unloading in order to compare these values with calculated values obtained by FEM analysis

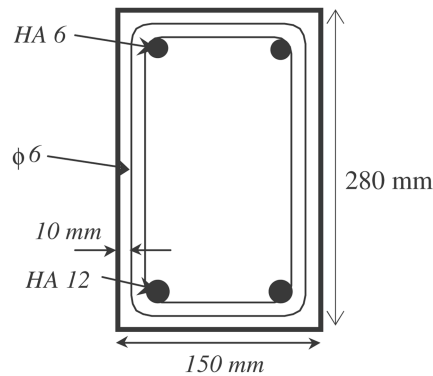


Fig. 2 Cross-section of the RC beams

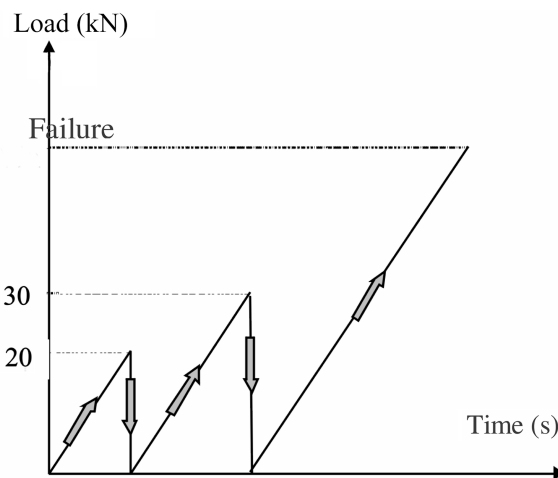


Fig. 3 Loading cycle

2.2. Test set-up

The location of the plastic tubes could induce a dissymmetrical behaviour, so deflections were measured at three positions of the beams (Fig. 4). Transducers have been placed to monitor the beam deflection with magnetic supports at three positions: mid span, 40 cm left of the mid span, and 40 cm right of the mid span. The outputs of the deflection transducers and applied load were connected to a recorder to plot the three load-deflection curves.

For the local analysis, the state of cracking was followed during the loading. The curvature of 7 cross sections (called A to G) was measured with a ball deformer (Fig. 5).

The curvature was determined by plotting the straight line best correlating the 4 deformations measured on the height of the beam (Fig. 6). The experiment showed an accuracy of $\pm 15 \mu\text{m}/\text{m}$ for this measurement.

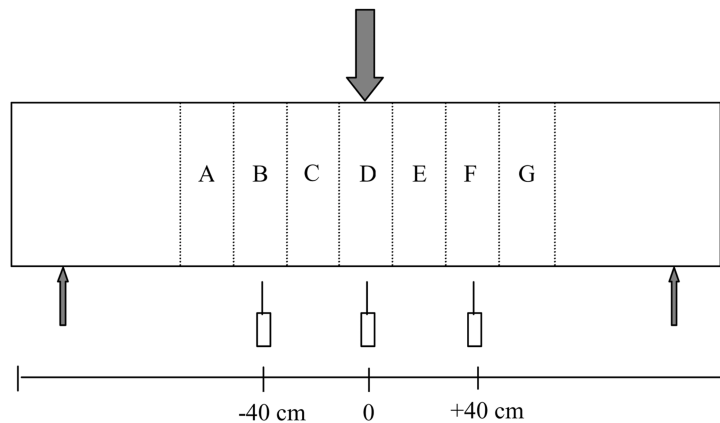


Fig. 4 Measurement of vertical deflection

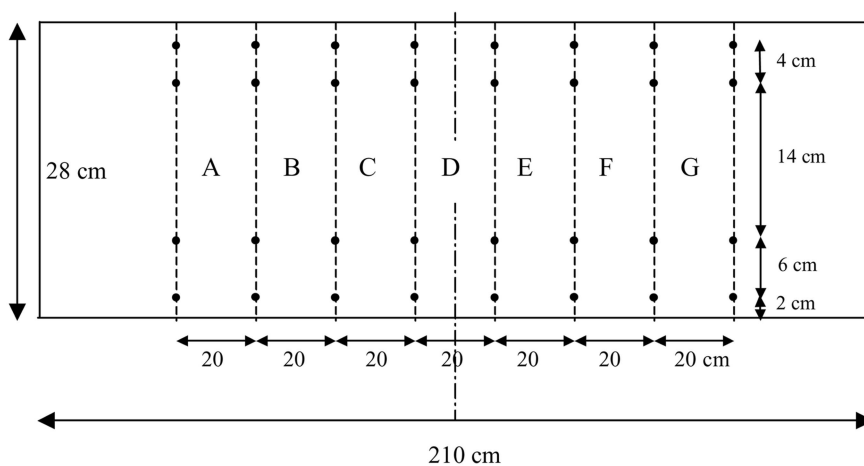


Fig. 5 Positions of the balls

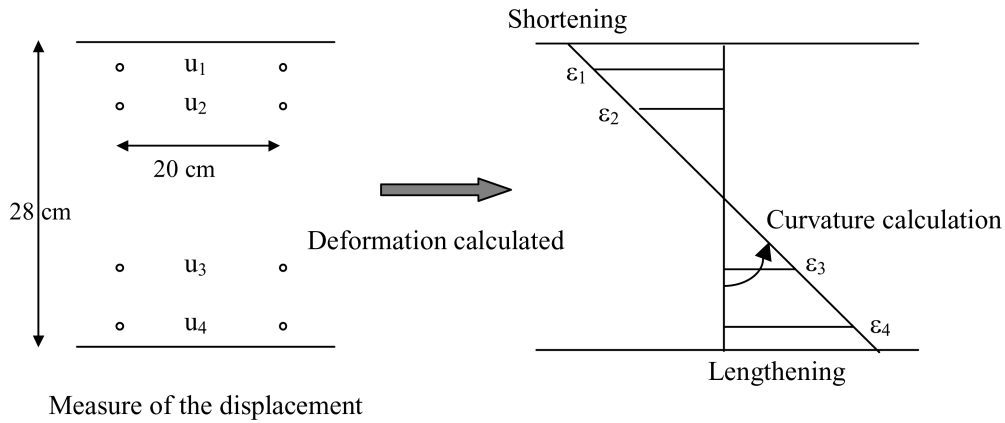


Fig. 6 Experimental determination of the curvature

3. Analysis of the flexural behaviour

3.1. Study of the flexural behaviour at global scale

Figs. 7, 8, 9 and 10 present respectively the load-deflection curves for the TEMOIN, ADHCE, ADHTO and ADHAP beams. The left curve presents the deflection at mid-span (C) while the right curve presents the deflection at 40 cm from mid-span (C±40). The cracking pattern for each beam is presented in Fig. 11.

For the TEMOIN beam a classical flexural behaviour has been observed (Fig. 7). The first cracking load was evaluated equal to 18 kN and cracking began to develop in the central part of the beam. For a load of 40 kN, shear inclined cracks appeared near the bearings. The failure by reinforcement yielding and compressed concrete crushing occurred for a load of 72 kN.

For the ADHCE beam, the bond was removed in the central part, from C-40 cm to C+40 cm. The first crack appeared near mid span at C-10 cm for a low load level of 5 kN. As for TEMOIN beam, at about 40 kN shear cracks appeared near the bearings, and one more bending crack but with a lower opening was observed at C+20 cm. This second bending crack in the unbonded zone was

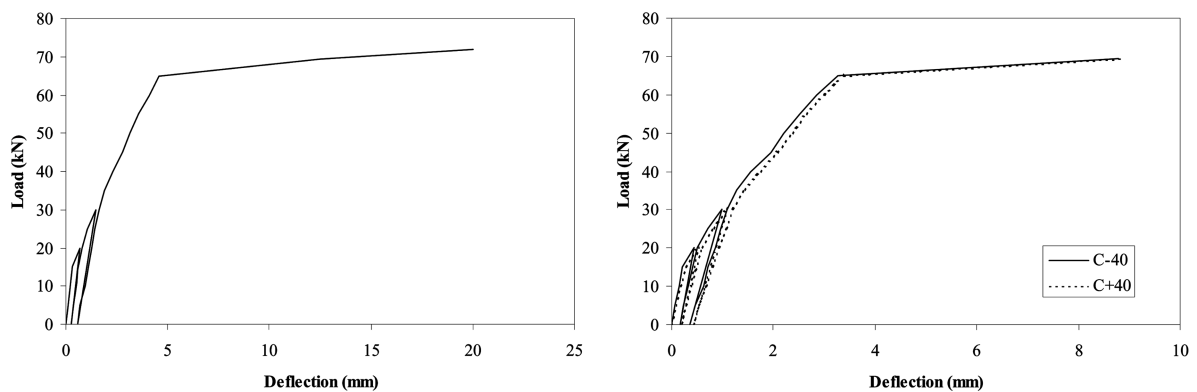
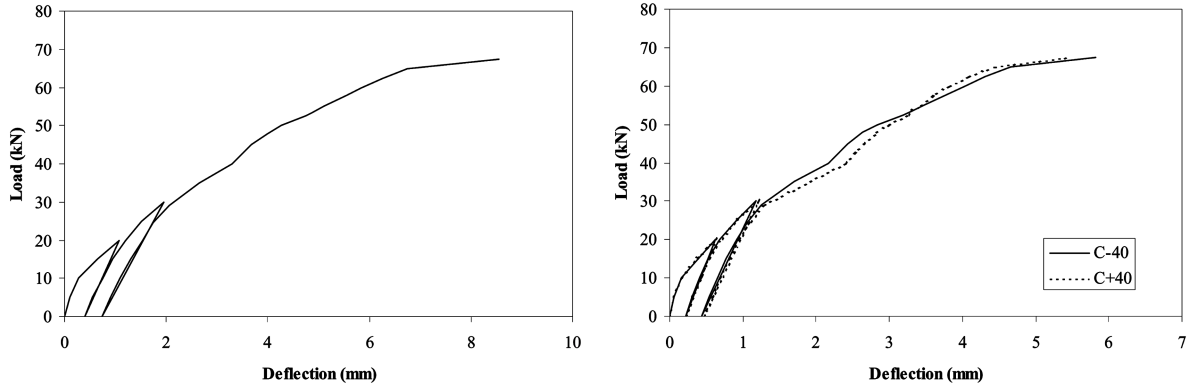
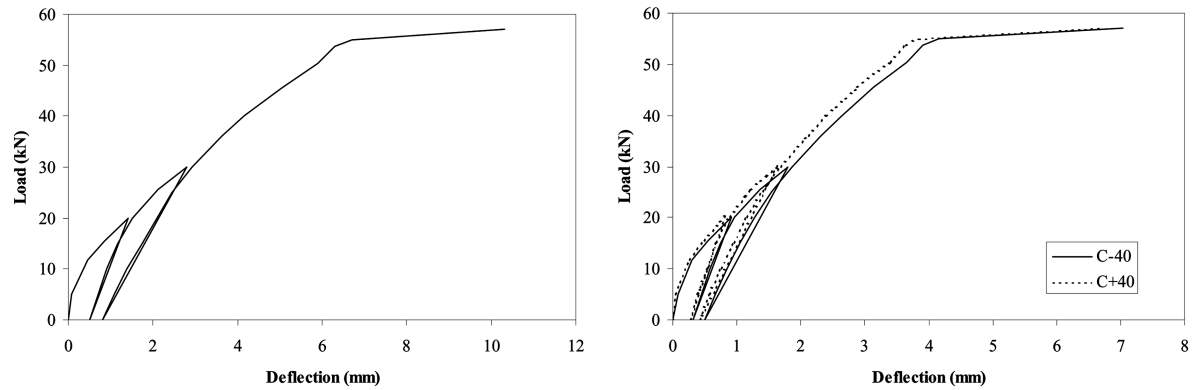
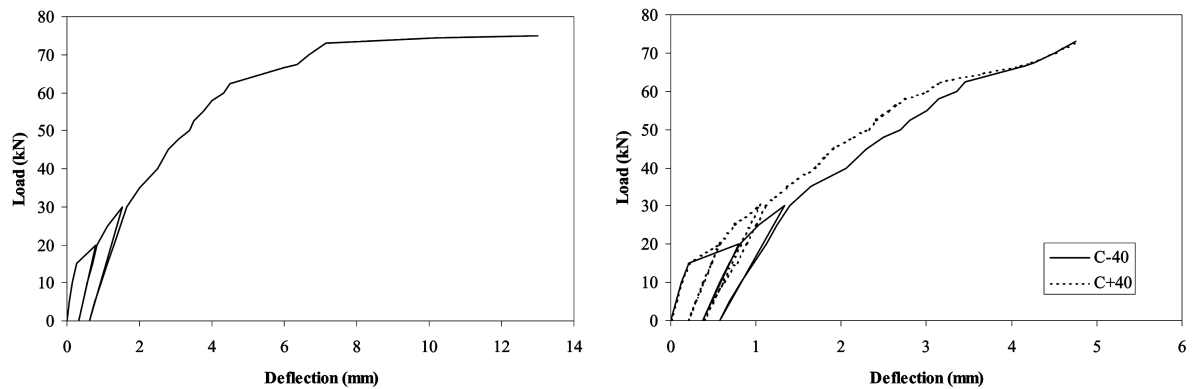


Fig. 7 Load deflection curves at mid-span and C±40 cm, TEMOIN beam

Fig. 8 Load deflection curves at mid-span and C \pm 40 cm, ADHCE beamFig. 9 Load deflection curves at mid-span and C \pm 40 cm, ADHTO beamFig. 10 Load deflection curves at mid-span and C \pm 40 cm, ADHAP beam

located at the level of a stirrup, and could be the result of a manufacturing defect. The failure by reinforcement yielding just followed by the crushing of the compressed concrete with a large opening of the first mid span crack occurred for a load of 67.4 kN (Fig. 8).

For the ADHTO beam, the bond was removed all along the longitudinal reinforcement. As for the

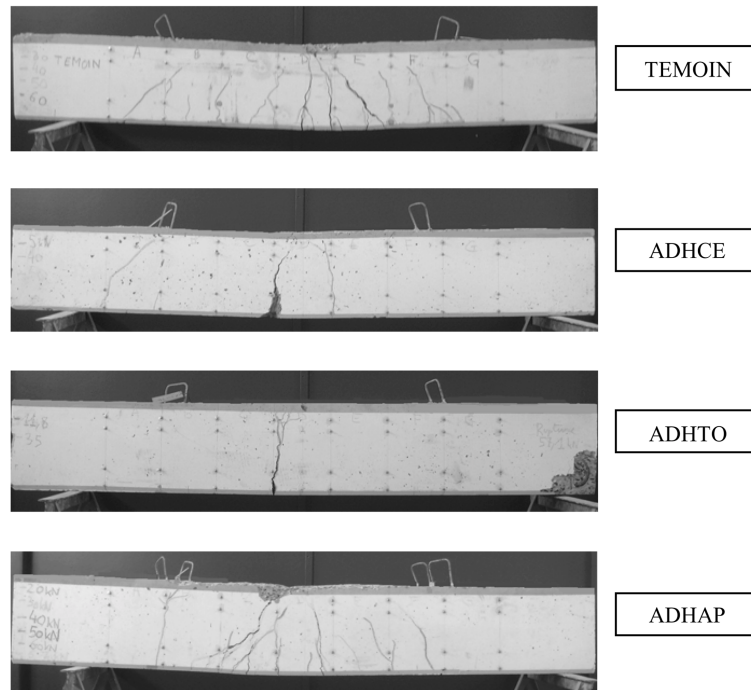


Fig. 11 Cracking pattern for bending test

ADHCE beam, the first and only crack appeared near mid span for a low load level of 8 kN. The stiffness of the right part of the beam was noticed higher than that of the left part, because this bending crack appeared near C+10 cm (Fig. 11 - ADHTO). The failure was initiated by the spalling of the concrete at the level of the right anchoring hook for a load of 57.1 kN, followed by crushing of the compressed concrete, without any shear cracks. (Fig. 9).

For the ADHAP beam, the bond was removed along 60 cm near the left bearing. The first crack was observed for a load of 17 kN in the part without bond (left part of the Fig. 11 ADHAP). At 25 kN, a bending crack appeared in the central part. Around 45 kN, the development of a shear cracks was observed between the mid span and the right end of the part without bond (Fig 11 ADHAP). It can be observed that the stiffness at C-40 cm is lower than the stiffness at C+40 cm (Fig. 10).

In Fig. 12, the load deflection curves at mid-span for the various tests are compared. In Table 1 are presented the main characteristics of these curves. The remove of bond in the central part has induced an earlier bending cracking for ADHCE and ADHTO beams, involving a decrease of flexural stiffness compared to the TEMOIN beam. For the ADHAP beam, the decrease of flexural stiffness was lower because the length without bond was less bended, and the cracking load was similar to that of the TEMOIN beam. The yielding load and the ultimate load were also similar for ADHAP and TEMOIN beams. On the other hand, the decrease of the ultimate load was about 6% for the ADHCE beam and about 20% for the ADHTO beam.

Moreover, it is interesting to note the increase of the deflection in relation to the TEMOIN beam, for 30 kN, 2% for ADHAP beam, 28% for ADHCE beam, and 81% for ADHTO beam. These results show the influence of the bond factor on the deflection. A general loss of bond will be more harmful than a local loss of bond in term of deflection.

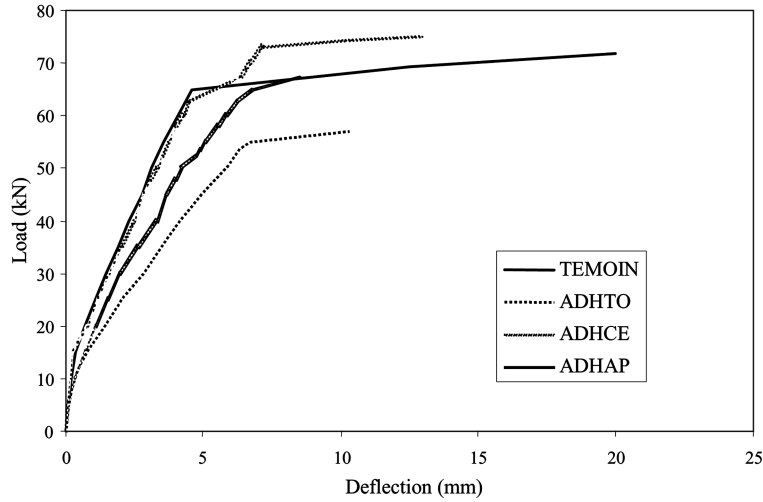


Fig. 12 Load-deflection curves at mid-span for all tests

Table 1 Main results

Beam	Cracking Load (kN)	Yielding Load (kN)	Ultimate Load (kN)	Deflection 30 kN (mm)
TEMOIN	18	65	72	1.61
ADHCE	5	65	67.4	2.06
ADHTO	8	53.7	57.1	2.92
ADHAP	17	62.5	75.1	1.65

Table 2 presents the evolution of the residual deflection for each test after unloading both at 20 and at 30 kN. These results allow appreciating the irreversibility and the level of damage of the beam. The loss of bond in the central part (ADHCE) has induced a low increase of the mid-span deflection (C). The same behaviour was observed for ADHTO beam with a higher increase, because the zone without bond is longer. For ADHAP, the increase at mid-span was lower, particularly more important at C-40 cm, because the bond was removed on this side.

3.2. Mechanical behaviour at local scale

The load-curvature curves are presented in Fig. 13. Five values of measures are presented respectively corresponding to a load of 20 kN, the first unloading, a load of 30 kN, the second

Table 2 Residual deflection after unloading at 20 and at 30 kN

Beam	Residual Deflection 20 kN (mm)			Residual Deflection 30 kN (mm)		
	C-40	C	C+40	C-40	C	C+40
TEMOIN	0.16	0.25	0.19	0.36	0.56	0.41
ADHCE	0.21	0.40	0.22	0.43	0.74	0.47
ADHTO	0.31	0.50	0.27	0.50	0.80	0.41
ADHAP	0.37	0.33	0.20	0.58	0.63	0.39

unloading and finally a load of 40 kN. The higher values are noticed for the ADHCE and ADHTO beams, with a curvature peak at mid-span. For ADHCE beam, the two cracks observed at the central part induced a broader distribution of curvature than for ADHTO. For ADHAP and TEMOIN beams, the values of the curvature were the same except for the left part of ADHAP beam where the bond was removed and where the main crack was developing.

3.3. Conclusion of the experimental study

This study allows to experimentally assess the effect of a localized loss of bond along longitudinal reinforcement. It has been noted that the decrease of the ultimate load is larger when the length of the zone without bond decreases. The same evolution is also observed for the deflection corresponding to a load of 30 kN. On the other hand, a loss of bond near the bearings induces only small changes in the behaviour.

The cracking also depends on the location of the loss of bond. When the zone without bond is central, the first crack load is significantly lower than for other tests, and the first crack is roughly central and developing into a large opening. Shear cracks can develop only in zones with bond. If the anchoring length of the bars is not sufficient, the failure is brittle and begins by a spalling of one end of the beam.

Now, it is interesting to evaluate the relation between a total loss of bond, as in the experimental study, and the corresponding degree of corrosion. Using a Finite Element, model with special

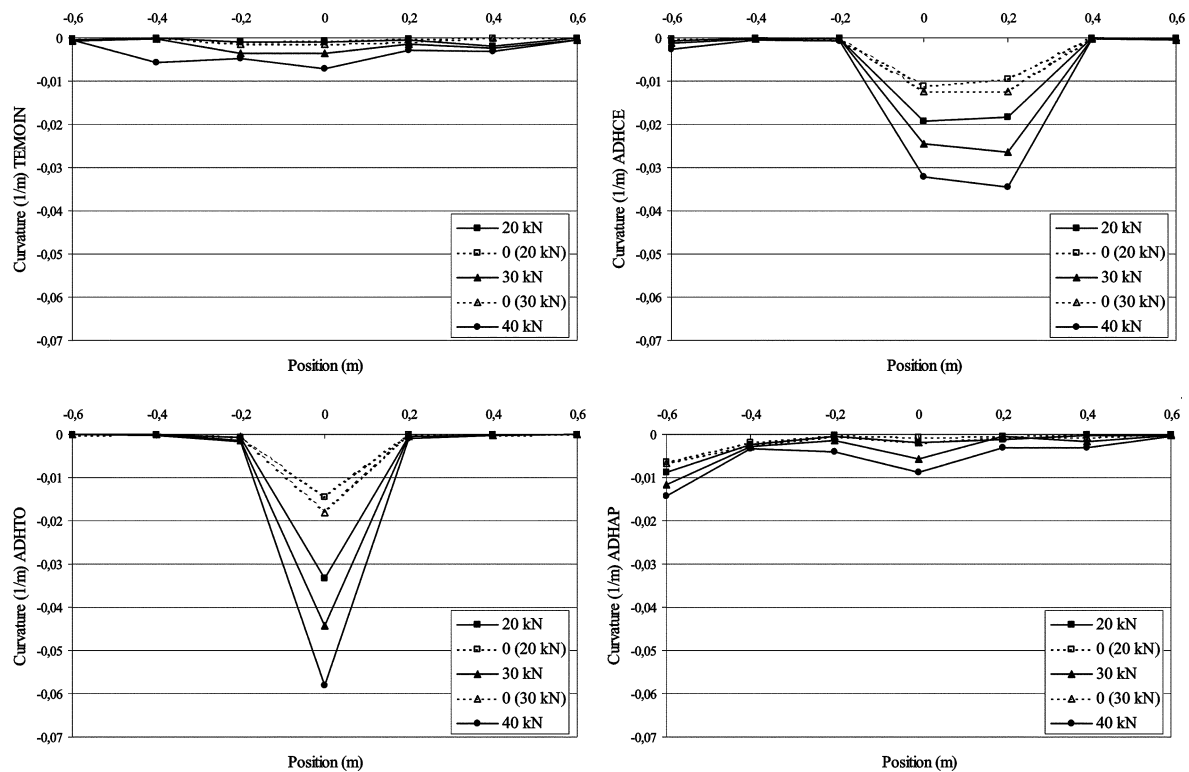


Fig. 13 Load-curvature curves

interface element named rust element allows evaluating this corresponding degree of corrosion. As in the experimental study, the effects of the corrosion will be simulated only by loss of bond and the corresponding degree of corrosion will be evaluated by fitting to experimental curves.

4. Finite element analysis of RC beams with degraded bond

4.1. Outline of FEM analysis

In this part, the loss of bond corresponding to the experimental simulations will be evaluated by a Finite Element calculation. A special interface element, called rust element, is used and placed in the mesh between the steel and the concrete to conduct a simplified analysis of local bond behaviour. The mechanical properties of the rust element are only related to the degree of corrosion. In a first time, the calculation will be made considering only the degradation of the steel-concrete interface, without any loss of the steel cross section, to evaluate the degree of corrosion corresponding to the total loss of bond. The cracking of concrete due to corrosion is not included in this calculation method.

4.2. Behaviour of materials

Behaviour of the concrete: The elastic-plastic model used is based on the smeared crack approach and is implemented in the finite element software CASTEM 2000.

Three criterions are used to describe the limit surface: Drucker-Prager for compression and bi-compression failure, and Rankine for tensile failure.

The failure model is based on plasticity with a negative work hardening in the direction of failure with a flow perpendicular to the rupture surface, which induce anisotropy. Three node triangle elements (TRI3) are used because the convergence is better than with four node elements (QUA4). The element size must not be too small, because in the local approach, the concrete cannot be considered as a homogeneous material at this level of resolution, and the smeared cracked approach concept is no longer valid. A lower size limit must be considered equal to $3d_a$, where d_a is the diameter of the coarser aggregate (Dekoster, *et al.* 2003).

Behaviour of the steel: An elastic-plastic model with isotropic hardening work is used. Two nodes linear bar elements are used. When the steel cross section reduction by corrosion is considered, the linear relation Eq. (2) is used:

$$A_c = A(1 - \eta) \quad (2)$$

A_c is the section after corrosion, A the section before corrosion, and η the degree of corrosion.

Behaviour of the interface: the interface is modelled with rust elements (Dekoster, *et al.* 2003), which are volume elements. The volume of the rust is more important than that of the original steel, generally assumed to be about two or three times. As the goal of this research program is to develop a simplified method to calculate corrosion effects on structural elements, pre-cracking corrosion was not taken into account. The rust production x_r is a function of the corrosion depth x , assuming in this study that the increase is twice the initial section Eq. (3). This assumption is not

acting upon the accuracy of the model, as proved in a previous parametric analysis (Dekoster, *et al.* 2003). Eq. (4) gives the relation between the rust production x_r , the original radius of reinforcement r_0 , and the degree of corrosion η .

$$x_r = 2x \quad (3)$$

$$x_r = 2r_0(1 - \sqrt{1 - \eta}) \quad (4)$$

For the Finite Element computation, the rust production is taken into account as a third material inserted between steel and concrete. This use of a volume element rather than un-dimensional interface elements is the main original aspect of the model. It needs only the knowledge of the degree of corrosion whenever interface elements need the knowledge of several and various parameters.

For the rust element, an elastic behaviour is chosen, and the mechanical characteristics are assumed as nearly equivalent to those of water (Molina, *et al.* 1993). The values are:

$$\nu_r = 0.49 \quad (5)$$

for Poisson's ratio (because a ratio of 0.5 is not usable in a FE computation) and

$$K_r = 2.0 \text{ GPa} \quad (6)$$

for bulk modulus.

So the calculated Young's modulus is very low, but non-null.

$$E_r = 3(1 - 2\nu_r)K_r \quad (7)$$

Rust and steel are considered as distinct materials and their areas can be changed with corrosion degree. First the cross section is reconstructed (Fig. 14).

Then for steel, the use of two nodes elements allows if necessary a direct change of the area with the degree of corrosion. This change will be only considered in part 4.5. For the rust layer, three nodes triangles are used, but their size cannot be changed in order to agree with the finite element theory. So an equivalent modulus E_{eqr} - Eq. (8) is used corresponding to the change of rust area, which is given by Eq. (9).

$$E_{eqr} = E_r \frac{S_r}{S_r} \quad (8)$$

$$S_r(\eta) = 2\pi[(r_0 + x)^2 - (r_0 - x)^2] = 8\pi r_0^2(1 - \sqrt{1 - \eta}) \quad (9)$$

When it is necessary to take into account the heterogeneity of the distribution of the corrosion along the bars, it is possible to define the size of the rust elements according to the section where the corrosion degree η_{\min} is the lowest.

These facilities are not used in the present study, where corrosion is supposed to be uniformly distributed, and the size of the rust element was fixed equal to 1 mm, after a parametric analysis (Dekoster, *et al.* 2003) having shown that the best accuracy was obtained with a small element size.

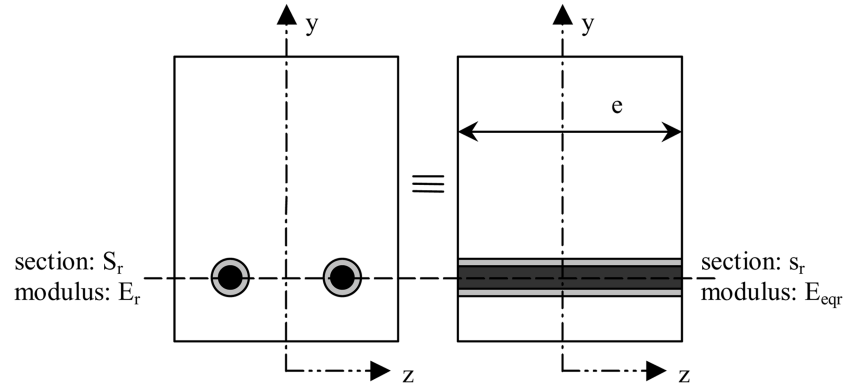


Fig. 14 Real and reconstructed cross section

4.3. Results of FEM analysis for the global behaviour

In Figs. 15, 16, 17 and 18 are presented respectively the experimental curve, noted EXP, and the calculated one, noted FEM, for TEMOIN, ADHCE, ADHTO and ADHAP beams. Except for the TEMOIN beam, the calculation is performed for various degrees of corrosion from 10% to 80%. In Fig. 15, it can be seen that the global behaviour is correctly evaluated by the finite element calculation for the TEMOIN beam. The results of the FE analysis for the different beams show that the loss of bond considered as the only effect of corrosion would be corresponding to a corrosion degree between 20% and 40% for the ADHCE beam (Fig. 16), and between 30% and 40% for the ADHTO beam (Fig. 17). For the ADHAP beam (Fig. 18), all the simulated curves are under the experimental curve.

These results induce that a corrosion degree between 20% and 40% is correctly corresponding to the total loss of bond. These results are similar to those of other studies (Stanish, *et al.* 1999). The results for the ADHAP beam show that a corrosion developed near bearings will not influence the global flexural behaviour.

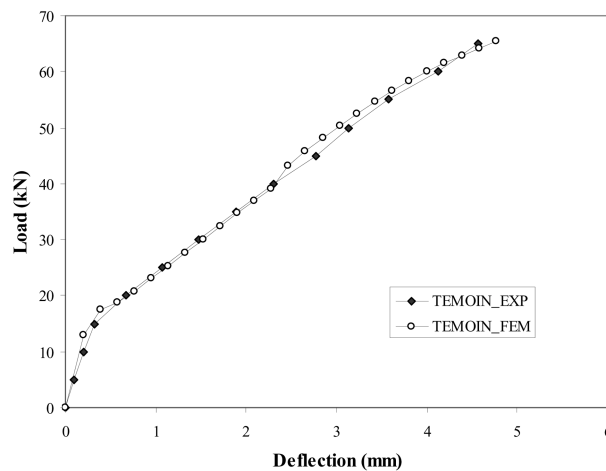


Fig. 15 Experimental and calculated load-deflection curves, TEMOIN test

4.4. Results of FEM analysis for the local behaviour

In Fig. 19 are presented the results of the calculation of the curvature for each beam. The comparison is made at a load level of 40 kN. The values of the curvatures for the TEMOIN,

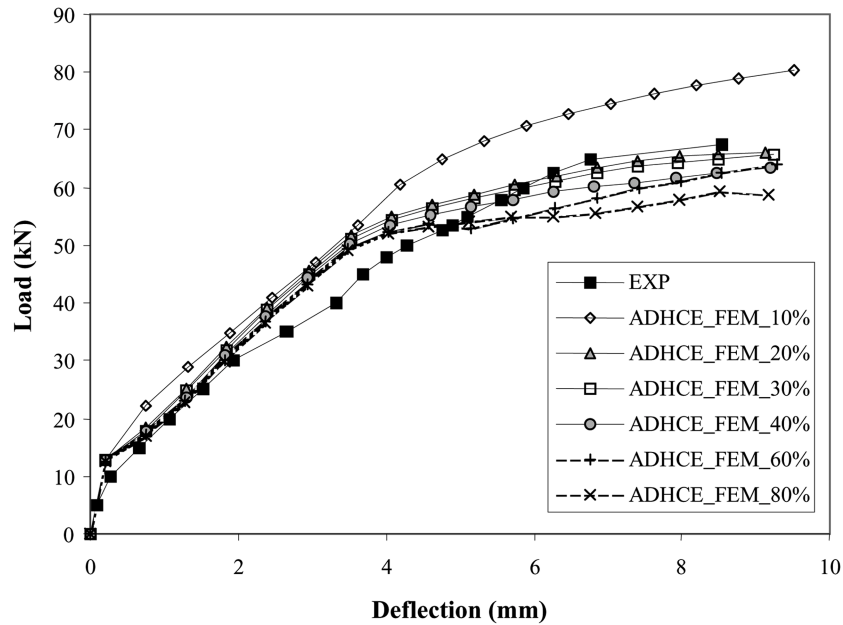


Fig. 16 Experimental and calculated load-deflection curves, ADHCE test

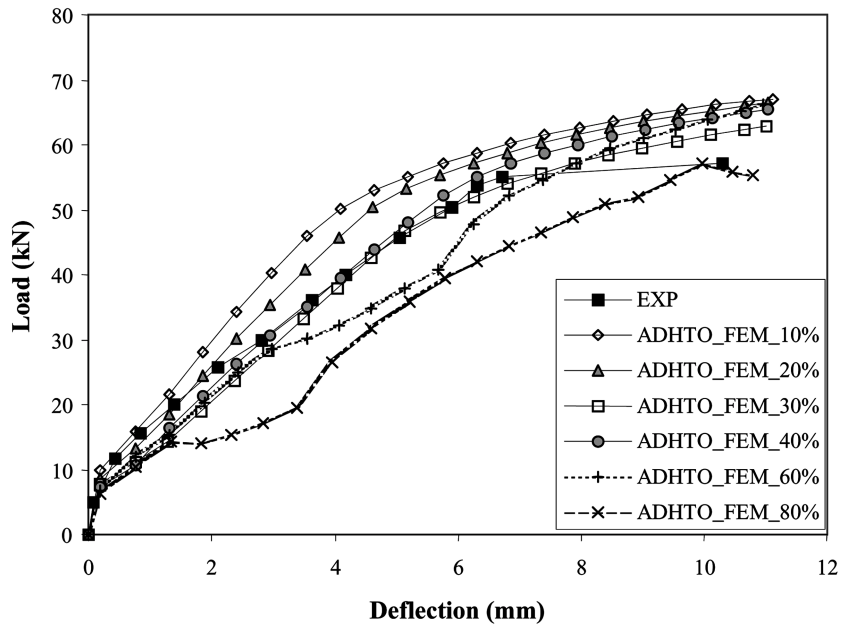


Fig. 17 Experimental and calculated load-deflection curves, ADHTO test

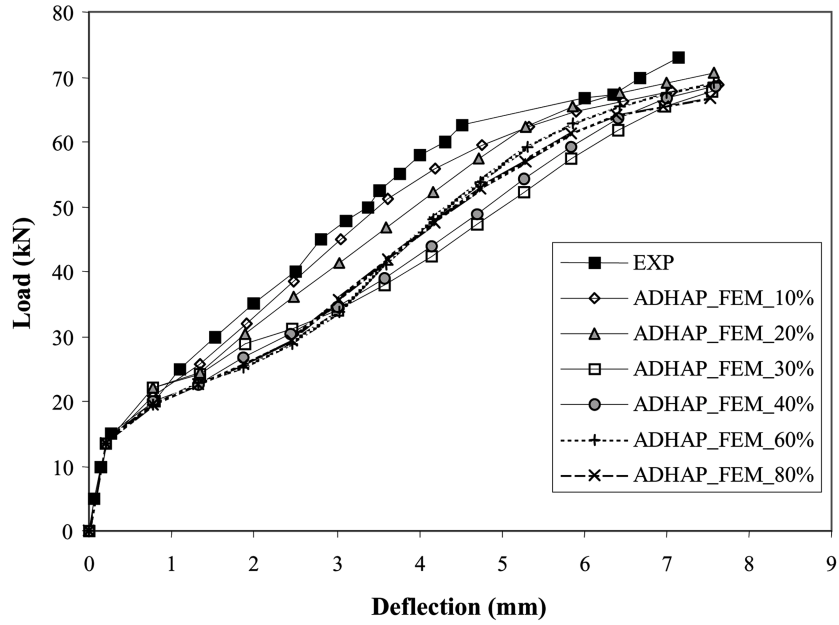


Fig. 18 Experimental and calculated load-deflection curves, ADHAP test

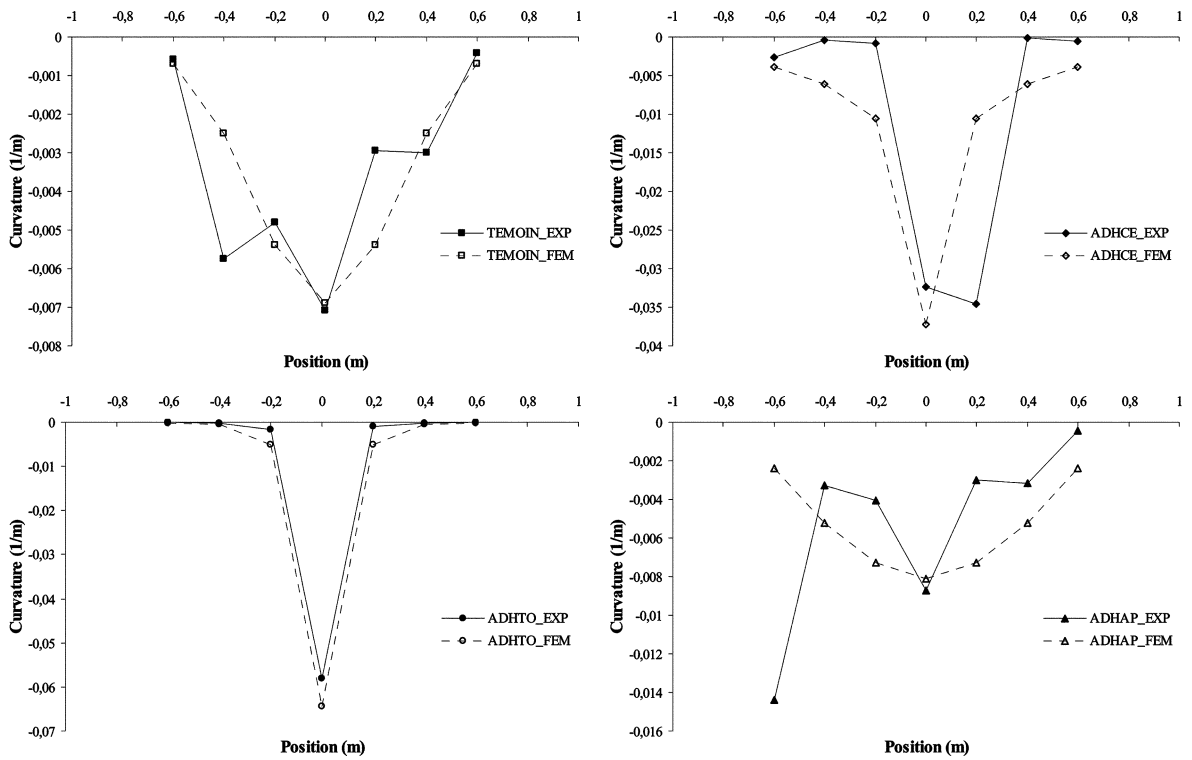


Fig. 19 Experimental and calculation curvatures comparison, for a loading of 40 kN

ADHCE and ADHTO beams are correct. The difference for each curve is due to the cracking pattern, because for calculation, the beam is assumed to be perfectly symmetrical and the concrete homogeneous. For the ADHAP beam the comparison is not correct. It can be explained by the use of the smeared crack approach for the Finite Element calculation, inducing a poor quality of the model when shear effects become predominant. As expected, the surface under the curves is about the same, showing that the integration of the local results on all the length of the beam tends toward a correct global behaviour evaluation.

4.5. Importance of the loss of bond (BL) and the loss of steel cross section (CSL)

The relation is now effective between a total loss of bond and the degree of corrosion with the regarded FE model. It can be interesting to complete this study by using a corrosion degree corresponding to this state, for example 30%, and simulating the experiments considering together the loss of bond and the loss of steel cross section. Figs. 20, 21 and 22 present respectively the comparison between the test with only loss of bond (BL) and the test with both loss of bond and loss of steel cross section (BL+CSL) for the ADHCE, ADHTO and ADHAP beams. The different results are presented in Table 3.

The results are interesting, enabling to identify the influence of each corrosion parameter (Dekoster and Buyle-Bodin 2003). For a corroded zone located near a bearing (ADHAP), the influence of the corrosion is not so important because the decrease of the ultimate load is only 9.7%. It can be noted that the loss of bond induces 71.1% of the decrease of the ultimate load. In this case, the corroded zone is far from the loading point and far from the maximum bending zone. For a corroded zone located at the central part of the beam (ADHCE), the decrease of the ultimate load is rather significant (34.6%) and induced mainly by the loss of steel cross section, for 71.1% of

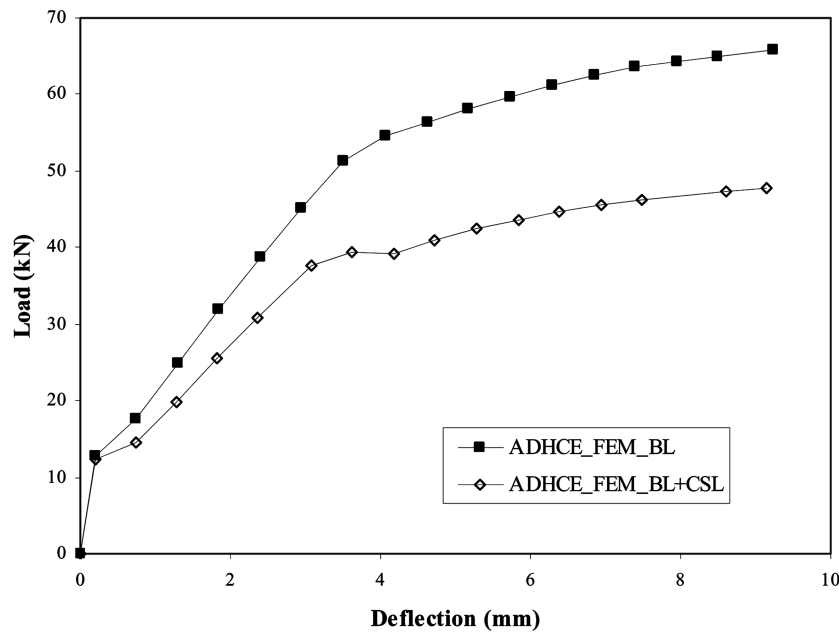


Fig. 20 BL and BL+CSL, ADHCE beam

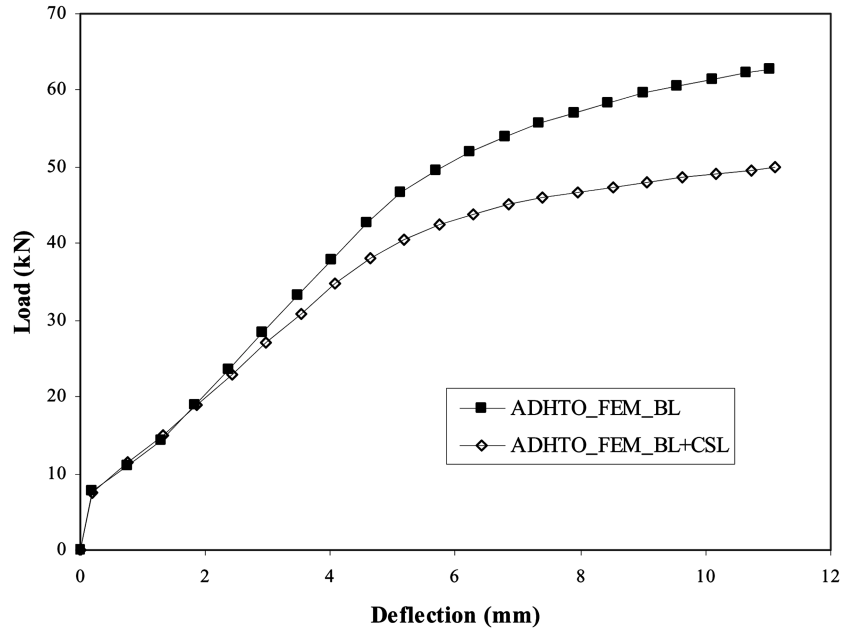


Fig. 21 BL and BL+CSL, ADHTO beam

the total decrease. In this case the corroded zone corresponds to the zone of maximum bending moment. For a corroded zone all along the reinforcement (ADHTO), the decrease of ultimate load is as important as for a localised corrosion (ADHCE), but the influence of each parameter is

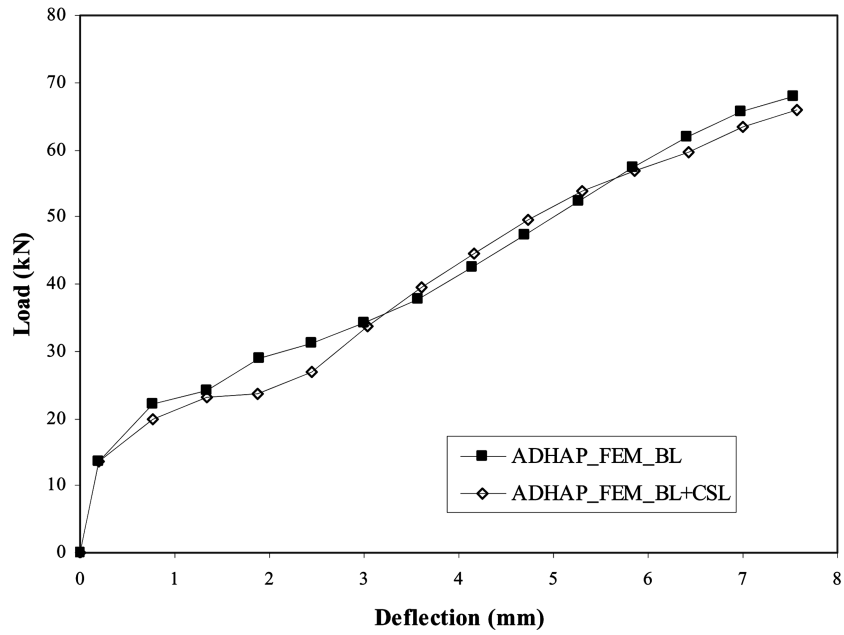


Fig. 22 BL and BL+CSL, ADHAP beam

Table 3 Influence of loss of bond and steel cross section vs. corrosion conditions

	Ultimate Load (kN) TEMOIN = 73 kN		Reduction of load compared to the TEMOIN ultimate load (%)		
	BL	BL+CSL	BL	BL+CSL	CSL
ADHCE	65.7	47.7	10.0	34.6	24.6
			28.9	100.0	71.1
ADHTO	62.8	49.8	13.9	31.8	17.9
			43.7	100.0	56.3
ADHAP	67.9	65.9	6.9	9.7	2.8
			71.1	100.0	28.9

different. The loss of bond induces a larger part (43.7%) of decrease, near that induced by the loss of section (56.2%).

These results are closely dependent on the model assumptions, and will need complementary experiments.

5. Conclusions

The effect of a total loss of steel-concrete bond on RC beams behaviour has been analysed. The parameter for the experimental study was the position and the size of the zone where the bond was removed. In a second stage, a finite element calculation has been performed using a special element, called “rust” element, in order to evaluate the percentage of corrosion corresponding to the total loss of bond. This comparison has led to a percentage of corrosion of 30%. This Finite element analysis does not take into account the corrosion-induced cracking.

Then a comparison on the finite element calculation only considering the loss of bond or considering both the loss of bond and the steel cross section reduction was led to an evaluation of the influence of each parameter in function of the corrosion conditions. Globally, a corroded zone located far from the loading point induces little consequence on the flexural behaviour (decrease of ultimate load about 10%) and the loss of bond is the more influent factor in this case. When the corroded and the loading zones are located at the same place, the decrease of the ultimate load is more important (about 35%), mainly induced by the loss of steel cross section. When the corrosion is developed all along the beam, the decrease of ultimate load is about 30%, but induced comparably by the loss of bond and the loss of steel cross section.

These results show that it will be interesting to conduct experimental studies and simulations of various cases of “real” corrosion, taking into account loss of bond and loss of steel cross section, and varying the position of the corroded zone along the beam, the size of this zone, the position of the loading point and the percentage of corrosion.

Acknowledgements

Grateful thanks to the French Commissariat à l’Energie Atomique (CEA) to allowing the use of the finite element code CASTEM 2000.

References

- Almusallam, A. A., Al-Gahtani, A. S., Aziz, A. R., Dakhil, F. H. and Rasheeduzzafar, A. (1996), "Effect of reinforcement corrosion on flexural behavior of concrete slabs", *J. Mater. Civ. Eng.*, **8**(3), 123-127.
- Al-Sulaimani, G. J., Kaleemullah, M., Basundul, I. A. and Rasheeduzzafar, A. (1990), "Influence of corrosion and cracking on bond behavior and strength of reinforced concrete Members", *ACI Struct. J.*, **87**(2), 220-231.
- Amleh, L. and Mirza, S. (1999), "Corrosion influence on bond between steel and concrete", *ACI Struct. J.*, **96**(3), 415-423.
- Cabrera, J. G. (1996), "Deterioration of concrete due to reinforcement steel corrosion", *Cem. Concr. Compos.*, **18**(1), 47-59.
- Castel, A., François, R., and Arliguie, G. (2000), "Mechanical behavior of corroded reinforced concrete beams Part 1: Experimental Study of corroded beams", *Mater. Struct.*, **33**(233), 539-544.
- Dekoster, M., Buyle-Bodin, F., Maurel, O. and Delmas, Y. (2003), "Modelling of the flexural behaviour of RC beams subjected to localised and uniform corrosion", *Eng. Struct.*, **25**(10), 1333-1341.
- Dekoster, M. and Buyle-Bodin, F. (2003), "Structural assessment of RC elements subjected to localised or general corrosion", *Proceedings of 2nd Int. Workshop on Life Prediction and Aging Management of Concrete Structures*, Paris, May, 115-26.
- Lee, H. S., Tomosawa, F. and Noguchi, T. (1998), "Fundamental study on evaluation of structural performance of reinforced concrete beam damaged by corrosion of longitudinal tensile main rebar by finite element method", *J. Struct. Constr. Eng.*, 506, 43-50.
- Molina, F. J., Alonso, C. and Andrade, C. (1993), "Cover cracking as a function of rebar corrosion: Part 2 Numerical model", *Mater. Struct.*, **26**(163), 532-548.
- Stanish, K., Hooton, R. D., and Pantazopolou, S. J. (1999), "Corrosion Effects on Bond Strength in Reinforced Concrete", *ACI Struct. J.*, **96**(6), 915-921.